Author(s): Sadi, Toufik & Kivisaari, Pyry & Tiira, Jonna & Radevici, Ivan & Haggren, Tuomas & Oksanen, Jani

Title: Electroluminescent cooling in intracavity light emitters: modeling and experiments

Year: 2017

Version: Post print

Please cite the original version:

Sadi, Toufik & Kivisaari, Pyry & Tiira, Jonna & Radevici, Ivan & Haggren, Tuomas & Oksanen, Jani. 2017. Electroluminescent cooling in intracavity light emitters: modeling and experiments. Volume 50, Issue 1. Optical and Quantum Electronics. 8. 0306-8919 (printed). DOI: 10.1007/s11082-017-1285-z.

Noname manuscript No.
(will be inserted by the editor)

Electroluminescent Cooling in Intracavity Light Emitters: Modeling and Experiments

Toufik Sadi · Pyry Kivisaari · Jonna Tiira · Ivan Radevici · Tuomas Haggren · Jani Oksanen

Received: date / Accepted: date

Abstract We develop a coupled electronic charge and photon transport simulation model to allow for deeper analysis of our recent experimental studies of intracavity double diode structures (DDSs). The studied structures consist of optically coupled AlGaAs/GaAs double heterojunction light emitting diode (LED) and GaAs p-n-homojunction photodiode (PD) structure, integrated as a single semiconductor device. The drift-diffusion formalism for charge transport and an optical model, coupling the LED and the PD, are self-consistently applied to complement our experimental work on the evaluation of the efficiency of these DDSs. This is to understand better their suitability for electroluminescent cooling (ELC) demonstration, and shed further light on electroluminescence and optical energy transfer in the structures. The presented results emphasize the adverse effect of non-radiative recombination on device efficiency, which is the main obstacle for achieving ELC in III-V semiconductors.

Keywords Electroluminescent Cooling · Intracavity Light Emitters · III-As · Light-Emitting Diodes · Photodiodes

1 Introduction

During the past couple of decades, research on planar optoelectronic devices involved less studies on conventional III-V based devices, and focused much

Toufik Sadi, Pyry Kivisaari, Jonna Tiira, Ivan Radevici, Tuomas Haggren and Jani Oksanen
Department of Neuroscience and Biomedical Engineering, Aalto University, P.O. Box 12200, FI-00076 AALTO, Finland
E-mail: toufik.sadi@aalto.fi

Pyry Kivisaari
Division of Solid State Physics and NanoLund, Lund University, P.O. Box 118, SE-22100 Lund, Sweden

more on devices based on nitrides and other emerging materials, such as antimonides and nanomaterials, by addressing the scientific and technological challenges introduced by these material systems [1], [2]. However, recent developments in optical cooling, light emission efficiency and information processing [3]−[5] is provoking a renewed interest in mature III-V materials, specifically III-As [6].

Two types of semiconductor-based optical cooling technologies have been predominantly studied in recent years: (i) laser cooling and (ii) electroluminescent cooling (ELC). Indeed, progress in solid-state cooling technologies has been pioneered by laser cooling of doped glasses [3] and semiconductors [7], and very low-power electroluminescent cooling of small bandgap light-emitting diodes (LEDs) has recently been demonstrated [8]. In general, photon emission of a semiconductor is dominated by photons with an energy higher than the bandgap (E_g). However, it is possible to create electron-hole pairs with an excitation energy that is smaller than E_g, with the remaining energy being drawn from lattice heat (thermal energy). Unlike laser cooling, where the excitation power quickly drops when the photon energy of the excitation drops below the bandgap energy, using an LED-based approach (with an electrical excitation) also allows using bias voltages and excitation energies that are well below the threshold set by the bandgap.

In principle, ELC at a high bias should be feasible with present materials (III-V semiconductors) but is yet to be reported. Despite considerable efforts, light confinement due to the large refractive index of typical semiconductors has remained a serious obstacle in demonstrating the optical cooling of semiconductors [9]. In practice, to achieve ELC, several general challenges need to be addressed, including reduced photon recycling and light extraction, device processing challenges, interface non-radiative recombination, non-uniform excitation effects and charge injection issues.

In order to achieve direct observation of cooling conditions, our most recent experiments [6] investigated the effect of enclosing a III-As light emitting diode and a light absorbing photodiode (PD) in an intracavity double diode structure (DDS) configuration, as illustrated in Fig. 1. This arrangement essentially eliminates the light extraction issues encountered in conventional setups. Furthermore, the presently studied intracavity approach can substantially relax the material requirements for reaching the high-current ELC regime. Also, electrical injection enables low bias operation. The integrated photodiode, providing current for the LED and thereby facilitating current spreading, allows direct measurement of the coupling quantum efficiency. Therefore, this structure can act as an extremely useful intermediate research prototype to demonstrate ELC and to investigate the main challenges associated with the demonstration. In practical terms, ELC can be demonstrated, if the condition $CQE(U) > U/\hbar\omega$ is met. In this case, CQE refers to the coupling quantum efficiency, defined as the ratio I_2/I_1 of the currents I_1 and I_2 through the LED and the PD, respectively, U is the potential drop across the LED and $\hbar\omega$ is the emitted photon energy. This condition indicates that the LED emits at least an optical power $I_2\hbar\omega/q$, while the injected electrical power is I_1U; if the

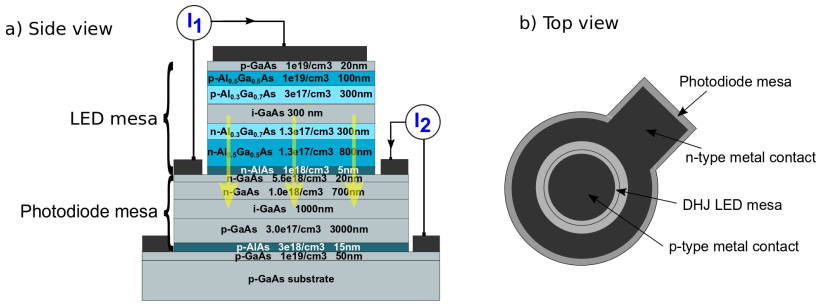

Fig. 1 An example of an intracavity DDS configuration, showing a) the typical layer arrangement (structure B_1) including materials and doping concentrations (side view), and b) a top view of the full 3D geometry.

emitted optical power is larger than injected electrical power, the LED cools down. Due to the lack of thermal insulation between the LED and the PD, however, these devices will not be able to produce significant temperature differences across the device without e.g. introducing vacuum nanogaps within the structure [10]. In this work, and backed by experiments, we apply the drift-diffusion (DD) formalism for electron charge transport, as coupled with a first order photon transport model, to understand further the behavior of the intracavity configuration, and to discuss its suitability for electroluminescent cooling.

2 Simulated structures and experimental setup

Fig. 1 shows the layer structure of our reference device (sample B_1), with an i-GaAs active layer (AL) of 300 nm. It incorporates a double heterojunction (DHJ) GaAs/AlGaAs LED grown on top of a GaAs p-n-homojunction photodiode. Light emission from the LED is guided towards the photodiode either directly or after reflection from the top contact. Direct measurements of the current components (Fig. 1) allows detecting the amount of absorbed light, as discussed in Ref. [6]. To support our simulation study, two measurement methods have been employed: (i) the four point probe $I-V$ measurement setup, to extract the $I-V$ characteristics of both the LED (I_1-V) and PD (I_2-V) and the corresponding coupled quantum efficiency (CQE) [6], and (ii) lock-in thermography and conventional luminescence microscopy methods [11], to probe emission patterns in the structure. In order to understand better the operation of the DDS, we consider various B_1 structures with different LED mesa diameters (100μm, 200μm, 500μm, 1mm). We also study two more structures B_2 and B_3, similar to structure B_1 (100μm mesa diameter), but with an AL of 50nm and 10nm, respectively.

3 Simulation Method

We employ a numerical transport model based on the DD current and continuity equations for charge carriers, effectively coupling the partial differential equations for the electrostatic potential ϕ and the quasi-Fermi levels E_{fn} and E_{fp} for electrons and holes, respectively, as given below:

$$\nabla \cdot (-\epsilon \nabla \phi) = q\,(p - n + N_d - N_a)\,, \tag{1}$$

$$\nabla \cdot \mathbf{J}_n = \nabla \cdot (\mu_n n \nabla E_{fn}) = qR, \tag{2}$$

$$\nabla \cdot \mathbf{J}_p = \nabla \cdot (\mu_p p \nabla E_{fp}) = -qR, \tag{3}$$

where n is the electron density in the conduction band, p is the hole density in the valence band, $\mathbf{J}_n$ and $\mathbf{J}_p$ are the electron and hole current densities, respectively. Also, N_d is the ionized donor density, N_a is the ionized acceptor density, R is the net recombination rate per unit volume, ϵ is the permittivity, q is the elementary charge, and μ_n and μ_p are the electron and hole mobilities, respectively. Further details about the model can be found in [12]−[14]. The recombination rate R is modeled using the well-known parameterized formula for radiative, Shockley−Read−Hall (SRH), Auger recombination [12], and surface and interface non-radiative recombination [15]. In contrast to typical LED models, our structure involves three terminals described by Dirichlet-form boundary conditions, biasing the LED in the customary manner, while short-circuiting the PD. The LED and the PD are optically coupled, as follows. The electron-hole (e-h) recombination term R_{LED} in the LED active region is coupled to an e-h generation term G_{PD} in the photodiode layers through the optical coupling constant (CC) χ and the relation $G_{PD} = \chi R_{LED}$. Measuring the CC is not very straight-forward. However, it can be estimated by calculating the reflection coefficient of the (top p-type LED) contact structure, as described in Ref. [6]. Using the refractive indices reported in Ref. [6] and literature, the CC is estimated to be 90% [6]. The 10% loss associated with the coupling constant accounts for the mirror losses in the metal contact and the non-transparent top 'cap' GaAs layer. The attenuation of light in the PD is presently approximated by the Beer-Lambert law given by the following relationship:

$$I = I_0 \exp(-\zeta d), \tag{4}$$

where ζ is the absorption coefficient, d is the light penetration depth, and I_0 is the intensity at reference position $z = 0$, matching the emission at the corresponding position in the LED. Improved photon transport models are currently being considered, such as our in-house optical model [16]−[18] to extract the reflection coefficients and Green's functions of the multi-layered structure. Ultimately, we aim to solve for the radiative transfer equation (RTE), to include more accurately photon transport along different paths and angles. Table 1 summarizes the most relevant parameters used in our calculations.

Table 1 The most relevant parameters used in our calculations. It is noteworthy that the value of the SRH-like recombination constant A, as used in the simulations, is extracted from measurements for each device sample. The table only shows the range for this fitting parameter, for the mesa diameters and layer thicknesses used in this work.

Parameter	Value/range
SRH recombination constant A	$10^6 - 10^9$ (s^{-1})
Radiative recombination constant B	$2{\times}10^{-10}$ (cm^3s^{-1}) [19], [20]
Auger recombination constant C	10^{-30} (cm^6s^{-1}) [21]
Absorption coefficient ζ	10^4 (cm^{-1}) [22]

4 Results and Discussion

Our simulation model has been carefully calibrated with measurements, as described above, for different mesa diameter sizes and active layer (AL) thicknesses. Fig. 2 shows LED (I_1-V) and photodiode (I_2-V) characteristics, and the corresponding CQE as a function of bias for a 500μm diameter, and the peak CQE (from experiments and simulations) and the extracted SRH constant, for different mesa diameters. Fig. 2 highlights how the CQE is higher at larger mesa diameters, where the effect of SRH and interface non-radiative recombination is reduced, as highlighted in Fig. 2(d). Fig. 3 shows the radiation recombination maps from simulations (side view) and experiments (top view), for example devices. Clearly, simulations and experiments show a similar trend for radiation recombination distribution, with the peak emission occurring near the top contact edge.

Further analysis of the simulation results show that the presently used model parameters give a peak LED IQE of approximately 90%, for the 500μm mesa diameter device studied here. The peak photodiode IQE is lower at around 75%, under short circuit conditions (for the same diameter). For the smaller mesa diameters considered here (100μm or 200μm), both IQEs become even smaller. These results suggest that, despite the short circuit operation, one of the largest bottlenecks in the DDS operation may in fact be the efficiency of the solar cell. In the present model, the efficiency dependence on the mesa diameter originates almost completely from surface recombination, which is included in the effective SRH recombination coefficient and becomes relatively more pronounced when the device surface-to-volume ratio increases for smaller mesa sizes.

To further demonstrate the effect of non-radiative interface recombination on efficiency, we show in Fig. 4 the variation of the CQE as a function of bias, and the corresponding peak CQE from experiments and simulations, for active layers of 300nm (B_1), 50nm (B_2) and 10nm (B_3) thicknesses, and a 100μm mesa diameter. Fig. 4 shows a clear trend of a decreasing peak CQE with a decreasing AL thickness. Our simulations indicate that this reduction in CQE at thinner ALs is a direct consequence of the increased importance of non-radiative recombination at the interfaces of the AL. In practice, the reduction of efficiency due to the relative increase in the interface recombination

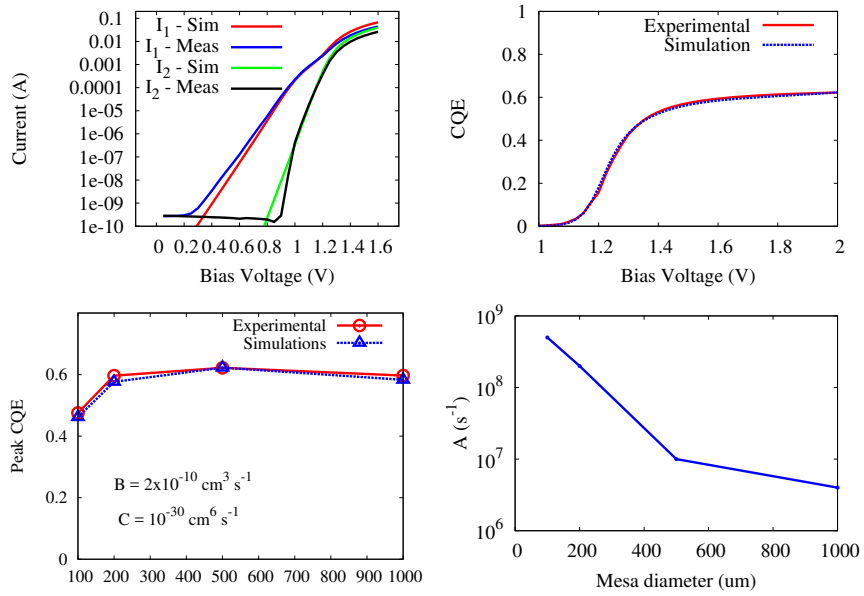

Fig. 2 (top-left) LED ($I_1 - V$) and photodiode ($I_2 - V$) characteristics, and (top-right) the corresponding CQE for a 500μm diameter, (bottom-left) the peak CQE from experiments and simulations, and (bottom-right) the extracted SRH constant, for different mesa diameters.

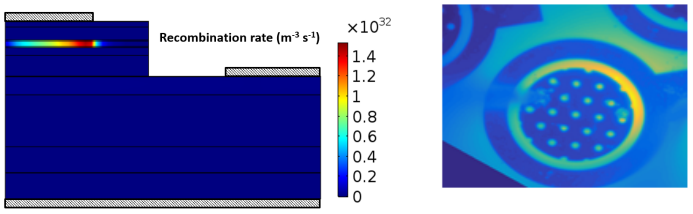

Fig. 3 Radiation recombination maps from (left) simulations (side view − for a mesa size of 100μm and a bias of 1.4V) and (right) experiments (top view − for a mesa size of 1000μm at a relatively high LED current).

is strongly affected by the interface and material quality, and it also competes with and is affected by several other effects such as current spreading, the Purcell effect and carrier densities at the interface. Therefore, while the present results suggest that thicker active regions work better for our structure, further work is in order to provide conclusive information on the optimal thickness of the active layer.

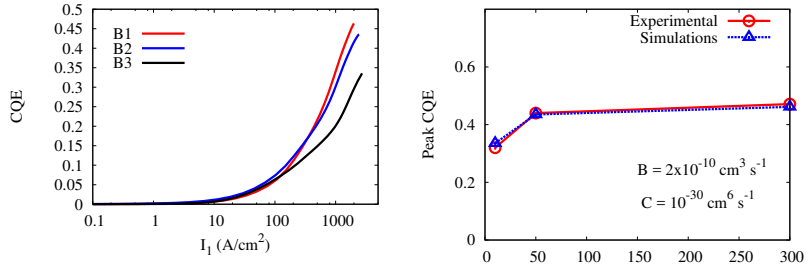

Fig. 4 The variation of the CQE as a function of LED current density, and the corresponding peak CQE from experiments and simulations, for a 100μm mesa diameter, and active layers of 300 (B_1), 50 (B_2) and 10 nm (B_3) thicknesses.

5 Conclusion

To conclude, we used the DD formalism with first order optical coupling, as supported by experiments, to study intracavity DDSs, as proof-of-concept devices with a strong potential for electroluminescent cooling. We presented results emphasizing how non-radiative recombination in the active layer and its GaAs/AlGaAs interfaces may affect device efficiency. This effect and other factors, such as current crowding, leakage outside the active layer, nonisotropic emission from thin ALs, and the decay length of recombination outside metal contacts and towards the device edges, may all contribute to the presently relatively low efficiency ($< 65\%$), which is the main obstacle for achieving EL cooling. In theory, a CQE approaching 100% can be achieved if the DDS structure, material composition and the epitaxial structure are highly optimized. In practice, the optimal structure is expected to be highly dependent on several factors such as the material properties and optical losses. Hence, future work is warranted to explore in more details these effects and also incorporate more advanced optical coupling models, to provide deeper insight into the physics of the light emitters, allowing the design of efficient solid-state EL cooling devices by optimizing the effect of geometrical features and material properties.

Acknowledgements We acknowledge funding from the Academy of Finland and the European Research Council under the Horizon 2020 research and innovation programme (grant agreement No 638173).

References

1. S. Nakamura and M. R. Krames, History of galliumnitride-based light-emitting diodes for illumination, Proc. IEEE, vol. 101, p. 2211, 2013.
2. M. Guina, A. Härkönen, V.-M. Korpijärvi, T. Leinonen, and S. Suomalainen, Semiconductor disk lasers: Recent advances in generation of yellow-orange and mid-IR radiation, Adv. Opt. Technol.,vol. 2012, Apr. 2012, Art. no. 265010.
3. M. Sheik-Bahae and R. I. Epstein, Optical refrigeration, Nature Photon., vol. 1, no. 12, pp. 693699, Dec. 2007.

4. J. Oksanen and J. Tulkki, Thermophotonics: LEDs feed on waste heat, Nature Photon., vol. 9, no. 12, pp. 782784, Nov. 2015.
5. D. Huang, P. Santhanam, and R. J. Ram, Low-power communication with a photonic heat pump, Opt. Exp., vol. 22, pp. A1650A1658, 2014.
6. A. Olsson, J. Tiira, M. Partanen, T. Hakkarainen, E. Koivusalo, *et al.*, Optical Energy Transfer and Loss Mechanismsin Coupled Intracavity Light Emitters, IEEE Trans. Elect. Dev., vol. 63, pp. 3567−3573, 2016
7. J. Zhang, D. Li, R. Chen, and Q. Xiong, Laser cooling of a semiconductor by 40 kelvin, Nature, vol. 493, no. 7433, pp. 504-508, 2013.
8. P. Santhanam, D. Huang, R. J. Ram, M. A. Remennyi, and B. A. Matveev, Room temperature thermo-electric pumping in mid-infrared light-emitting diodes, Appl. Phys. Lett., vol. 103, no. 18, p. 183513, 2013.
9. D. A. Bender, J. G. Cederberg, C. Wang, and M. Sheik-Bahae, "Development of high quantum efficiency GaAs/GaInP double heterostructures for laser cooling," Appl. Phys. Lett., vol. 102, p. 252102, 2013.
10. J. Oksanen and J. Tulkki, "Thermophotonic heat pump − a theoretical model and numerical simulations," J. Appl. Phys., vol. 107, p. 093106, 2010.
11. I. Radevici, J. Tiira, and J. Oksanen, "Lock-in thermography approach for imaging the efficiency of light emitters and optical coolers", SPIE Proc. 10121, no 101210Q, 2017
12. P. Kivisaari, J. Oksanen, J. Tulkki, and T. Sadi, "Monte Carlo simulation of hot carrier transport in III-N LEDs," J. Comput. Electron., vol. 14, pp. 382−397, 2015.
13. P. Kivisaari, T. Sadi, J. Li, P. Rinke and J. Oksanen, "On the Monte Carlo Description of Hot Carrier Effects and Device Characteristics of III-N LEDs," Advanced Electronic Materials, vol. 3, Art. no. 1600494, 2017.
14. T. Sadi, P. Kivisaari, J. Oksanen, J. Tulkki, "On the correlation of the Auger generated hot electron emission and efficiency droop in III-N light-emitting diodes," Appl. Phys. Lett., vol. 105, p. 091106, 2014.
15. Y. Chen, P. Kivisaari, M.-E. Pistol and N. Anttu, "Optimization of the short-circuit current in an InP nanowire array solar cell through opto-electronic modeling," Nanotechnology, vol. 27, 435404, 2016
16. T. Sadi, J. Oksanen, and J. Tulkki, "Effect of plasmonic losses on light emission enhancement in quantum-wells coupled to metallic gratings," Journal of Applied Physics, vol. 114, p. 223104, 2013.
17. T. Sadi, J. Oksanen, and J. Tulkki, P. Mattila, and J. Bellessa, "The Greens function description of emission enhancement in grated LED structures," IEEE Journal of Selected Topics in Quantum Electronics, vol. 19, p. 7800209, 2013.
18. T. Sadi, J. Oksanen, and J. Tulkki, "Improving light extraction from GaN light-emitting diodes by buried nano-gratings," IEEE Journal of Quantum Electronics, vol. 50, pp. 141−147, 2014.
19. V. P. Varshni, Phys. Status Solidi 19, "Band-to-Band Radiative Recombination in Groups IV, VI, and III-V Semiconductors (I)", vol. 2, pp. 459−514, 1967.
20. V. P. Varshni, Phys. Status Solidi 20, "Band-to-Band Radiative Recombination in Groups IV, VI, and IIIV Semiconductors (II)", vol. 1, pp. 9−36, 1967.
21. U. Strauss, W. W. Rühle, and K. Köhler, "Auger recombination in intrinsic GaAs," Appl. Phys. Lett., vol. 62, no. 1, pp. 55−57, 1993.
22. H. C. Casey, D. D. Sell, and K. W. Wecht, "Concentration dependence of the absorption coefficient for n- and p-type GaAs between 1.3 and 1.6 eV", J. Appl. Phys. 46, vol. 1, p. 250, 1975.